2020 IEEE/RSJ International Conference on Intelligent Robots and Systems (IROS)
October 25-29, 2020, Las Vegas, NV, USA (Virtual)

Stable Crawling Policy for Wearable SuperLimbs Attached to a Human with Tuned Impedance

Phillip H. Daniel[1] and Harry H. Asada[1]

***Abstract*— A control algorithm that allows a human model to crawl using a pair of supernumerary robotic limbs (SuperLimbs) is presented. The human model and SuperLimbs are coupled by a compliant harness. This work is inspired by the need for wearable robotic systems that can support workers engaged in fatiguing tasks. The walking policy is developed based on Lyapunov analysis. The volume of the region of attraction (ROA) of the system is used to quantify robustness and identify the optimal harness compliance. Simulation experiments are used to verify the performance of the algorithm. The presented formulation allows us to guarantee stable locomotion under nominal conditions and define robustness against modeling error and perturbations. This study is also the first, that the authors are aware of, to address cooperative crawling between a human and a wearable robotic system with state feedback.**

I. INTRODUCTION

Non-fatal construction industry injuries cost the US $7 billion per year [1]. Over-exertion accounts for over 23% of the most disabling U.S. workplace injuries [2]. This injury category includes injuries related to lifting, holding, or carrying objects. Poor ergonomics while doing these tasks can further exacerbate the problem. Welding jobs are an example career that is susceptible to these injuries and costs. Fig. 1 shows some of the poor postures that welders take while working.

Because of the high costs, there is increasing interest in wearable robots that augment the physical abilities of factory workers. Humans and robots are physically coupled in these systems, making dynamic interactions between each other.

In robotics and control literature, dynamics and control of legged robot systems have been studied extensively. These include both biped systems [3]–[6] and quadruped systems [7]–[9]. Powered exoskeletons are also extensively studied. These have actuators attached to the joints of the human body to increase muscular strength [10], [11].

Fig. 1 shows a new type of wearable robot, called Supernumerary Robotic Limbs, or SuperLimbs for short. The left panel shows a human working on the floor being supported by a pair of SuperLimbs attached to their back. Note that the human can use both hands for their task while being supported by the SuperLimbs. This removes strain from their lower back. Research studying how to best support the operator while working in place was done by [12].

*This work was supported by the Centers of Mechanical Engineering Research and Education at MIT and SUSTech.

[1]Phillip H. Daniel and H. Harry Asada are with Department of Mechanical Engineering, Massachusetts Institute of Technology, Cambridge, MA 02139, USA docphil@mit.edu, asada@mit.edu

Fig. 1. SuperLimb supporting a human working on the floor (left) [12] and welders in ergonomically poor postures while working (right) [13]

The wearable SuperLimbs, as illustrated in Fig.1, differ from powered exoskeletons in that the robotic devices are not attached along the human limbs, but can take arbitrary postures independent of the human posture. This independence allows the SuperLimbs to create new functions and improved performance over exo-skeletons, however their dynamics and control problems are fundamentally different.

The SuperLimbs are also different from traditional quadruped robots, where all four legs are controlled with a centralized controller creating a coordinated gait pattern. The four legs formed by the human and the SuperLimbs are controlled by a mixture of two different controllers; human and robot controllers.

This work presents a cooperative crawling policy for the SuperLimbs. This extends the functionality of the platform beyond the work done in [12] by allowing the operator to complete bi-manual tasks while simultaneously crawling and regulating their posture.

A dynamic coupler is inserted at the interface of the human and SuperLimbs. Simulation experiments are used to show that their is an optimal impedance for this coupler that maximizes the robustness of the gait control system.

First we describe existing work and highlight how it differs from the SuperLimb system. Then we describe a SuperLimb policy that uses the full system's state to crawl. This formulation allows us to specify necessary conditions for stable locomotion. We then demonstrate the policy's behavior with simulation experiments and comment on the impact of interface compliance on its stability. We conclude by sharing our plan for future work.

Standard linear quadratic regulators (LQR) are a major component of the presented policy. We show how they can be used in a novel way to coordinate the motion of the Human-SuperLimb system and guarantee stable locomotion.

II. PRIOR ART

The interface between a human and exo-skeleton is often modeled as a mass-spring-damper system [10], [14] that connects the human's displacement to the exo-skeleton's. This compliance represents the compliance of the human tissue and any external padding between the human's skeleton and the exo-skeleton's force sensor. Controlling the interface force with feedback is equivalent to controlling the interface displacement.

It is widely known that this control problem leads to instability at high gains [15], [16]. If we consider the simple linear model studied in [17], we can gain some insight into the cause of this shortcoming. [17] models a human arm grabbing the force sensor attached to the endpoint of a robotic limb, but this is analogous to studying the dynamics of a human arm in an exo-skeleton.

We know from [17] that the system is conditionally stable with respect to the gain of the exoskeleton's force control law due to the non-collocation of the actuation and sensing. In general such system's maximum bandwidth increases (for a fixed phase margin) as the interface stiffness approaches the stiffness of the exo-skeleton structure, and decreases beyond this. This implies that exo-skeleton systems perform better the higher the interface stiffness is. Because there is an upper limit to the interface stiffness based on the compliance of human flesh, there is a fundamental limit to the achievable bandwidth of exo-skeleton systems. The dynamics of exo-skeleton assisted walking are complex and not explicitly discussed here, however it should be clear that bandwidth limitations due to interface compliance will also degrade the performance of this task as well.

Control schemes other than direct force control exist, however they either lack an explicit stability analysis or were found to be unstable when implemented [10], [11]. Direct force control has been shown to yield stable operation at constrained bandwidths [14], [18], [19].

Enforcing passivity has been shown to yield stable performance between interacting systems. Furthermore, this condition can be studied analytically [20]. Unfortunately, this constraint may not apply to human limbs because they may be active in nature. [21] proposes a framework for analyzing the stability of human-robot interactions and designing control policies. This method has not, to our knowledge, been extended to multi-degree of freedom robots such as lower limb exo-skeletons though.

Interface compliance's intrinsic limitation to control bandwidth has not been addressed in lower-limb exoskeleton systems, however the structure of the SuperLimbs allow us to address this challenge as discussed in the proposed policy.

The authors have not found work describing active systems for completing ground level tasks outside of the work of [12] and [22]. These studies primarily address stationary tasks, thus the results presented here address a different issue. Passive systems are commercially available for helping workers complete ground level work, such as [23]. These systems improve worker ergonomics while allowing for mobility, but they can not effectively adapt to different tasks. The presented work does not discuss obstacle avoidance, but it is feasible to imagine an updated policy with foot placement constraints that allow the SuperLimbs to navigate obstacles.

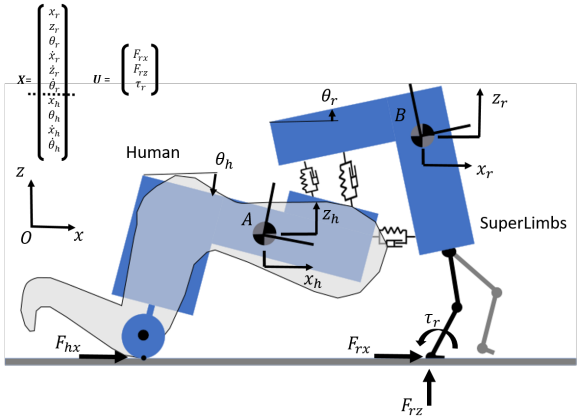

Fig. 2. System model with state and input vector shown

III. SYSTEM MODEL

We consider the system shown in Fig. 1 (Left), where the SuperLimbs are supporting the upper body of the human. We simplify the problem by modeling the sagittal plane dynamics only. The human crawls forward or backward by pushing towards the intended direction with their knees. The SuperLimbs are to react by taking steps and actively stabilizing the human during transit.

The human is a non-autonomous system with a reference state and a biological control policy that tracks it. Complex bio-mechanical modeling is beyond the scope of the current work. Instead we assume a simple dynamical model relevant to the operator's crawling motion.

Fig. 2 shows a schematic of the system consisting of a simple human model, a pair of SuperLimbs, and the dynamic coupler connecting them. The human is modeled as a single rigid body with a traction force F_{hx} at the knees. This traction force is assumed to be governed by the policy,

$$x_{h,error} = x_{h,desired} - x_h$$

$$\dot{x}_{h,error} = \dot{x}_{h,desired} - \dot{x}_h$$

$$F_{hx} = k_{p,cart} \cdot x_{h,error} + k_{c,cart} \cdot \dot{x}_{h,error}. \qquad (1)$$

$x_{h,desired}$ is the desired position of the human's Center of Mass (CoM), $\dot{x}_{h,desired}$ is their desired speed, and $k_{p,cart}$ and $k_{c,cart}$ are PD gains. In this formulation the height of the human's CoM is not actively controlled.

The SuperLimbs are modeled as a pair of mass-less legs attached to a rigid body. These legs make ground contact with no impulsive forces, weight switches between feet instantaneously so that the system is always in single support, and we assume that the feet do not slip. Each leg has three actuators driving the hip, knee and ankle joints. Actuator saturation is neglected in this analysis. We consider crawling

on flat ground only. The coupler consists of three pairs of springs and dampers; two for translational displacements and the third for rotational displacement.

The system's state, $X \in \mathbb{R}^{10}$, consists of the x-position of the human's CoM x_h, the orientation of the human body θ_h, the x and z-position of the biped's CoM x_r and z_r, the orientation of the biped's body θ_r, and their time derivatives. The legs are not part of the state because they are massless. The wheel generating the human traction force is assumed to be in contact with the ground at all times, and we assume that it does not slip. The system's input vector, $U_{total} \in \mathbb{R}^3$, consists of the x and z-directed forces of the biped's foot F_{rx} and F_{rz}, and torque from its ankle τ_r. The state and input vectors are illustrated in Fig. 2. Frame "O" is the inertial reference frame, and frames "A" and "B" are body frames fixed to each body's CoM. $r_{ft,x}$ is the x-component of the vector to the biped's ground contact point.

The coupler generates the wrench,

$$F_{coup} = \begin{bmatrix} F_{c,x} \\ F_{c,z} \\ \tau_c \end{bmatrix} = {}^{O}R_A \cdot (K \cdot \Delta r + D \cdot \Delta \dot{r}). \quad (2)$$

$$K = \begin{bmatrix} k_x & 0 & 0 \\ 0 & k_z & 0 \\ 0 & 0 & k_\theta \end{bmatrix}$$

$$D = \begin{bmatrix} d_x & 0 & 0 \\ 0 & d_z & 0 \\ 0 & 0 & d_\theta \end{bmatrix}$$

$$\Delta \dot{r} = \begin{bmatrix} {}^{A}\Delta \dot{X} \\ {}^{A}\Delta \dot{Z} \\ \Delta \dot{\theta} \end{bmatrix}$$

$$\Delta r = \begin{bmatrix} {}^{A}\Delta X - {}^{A}\Delta X_{naturallength} \\ {}^{A}\Delta Z - {}^{A}\Delta Z_{naturallength} \\ {}^{A}\Delta \theta - {}^{A}\Delta \theta_{naturallength} \end{bmatrix}$$

K, D, Δr and $\Delta \dot{r}$ are the stiffness, damping, relative displacement and relative velocity of the bodies. $F_{c,x}, F_{c,z}$, and τ_c are the x and y-directed coupling forces with respect to the inertial frame, as well as the coupling moment. The total system is control-affine of the form,

$$\dot{X} = f(X) + g(X) \cdot U. \quad (3)$$

$f(X)$ and $g(X)$ are nonlinear functions that depend on the parameters of the system such as $r_{ft,x}$.

IV. FORMULATION OF FULL STATE POLICY

We assume that the SuperLimbs have a measurement of the full state and knowledge of the human's reference position and velocity. This allows us to treat the system as autonomous and develop a robust crawling policy.

A closed form solution for equilibrium posture X_{eq} and input U_{eq} of the system is found such that $\dot{X} = 0$. The system has five unknown states and three independent inputs. There are five non-trivial equations of motion, so a combination of three of the states and inputs must be specified to yield a unique equilibrium. We choose to solve,

$$0 = f(X_{eq}) + g(X_{eq}) \cdot U_{eq}, \quad (4)$$

for X_{eq} and U_{eq} such that $\theta_{h,eq} = \theta_{r,eq} = \tau_r = 0$. This means that the human has a straight back and the ankle is applying no torque.

Next, we linearize the dynamics around this unique equilibrium. A_{lin} and B_{lin} are the linearized dynamic equations.

$$\Delta X = X - X_{eq}$$

$$\Delta U = U - U_{eq}$$

$$A_{lin} = \left[\frac{\partial f(X)}{\partial X} + \frac{\partial g(X)}{\partial X} \cdot U \right] \Bigg|_{X_{eq}, U_{eq}}$$

$$B_{lin} = g(X) \Big|_{X_{eq}}$$

$$\dot{X} \approx A_{lin} \cdot \Delta X + B_{lin} \cdot \Delta U \quad (5)$$

We design a Linear Quadratic Regulator (LQR) to stabilize the system around the equilibrium. A standard cost function is used,

$$C = \int_0^\infty \Delta X' \cdot Q \cdot \Delta X + \Delta U' \cdot R \cdot \Delta U dt. \quad (6)$$

Weighting matrices $Q \geq 0$ and $R > 0$. The algebraic Riccati equation is solved to yield a control policy of the form,

$$\Delta U = -G \cdot \Delta X. \quad (7)$$

$$G = R^{-1} \cdot B'_{lin} \cdot S \quad (8)$$

S is the positive definite solution of the Continuous Algebraic Ricotti Equation. We combine Eqs 5 and 7 to confirm asymptotic stability of the linearized system. This implies local asymptotic stability (LAS) of the non-linear system.

The equilibrium specified by Eqn 4 only satisfies the state and input conditions. This equilibrium does not imply that $x_{h,error} = 0$. In order to control the biped's gait, and thereby $x_{h,error}$, we propose to use successive linear controllers to stabilize the system while steps are commanded.

The Human+SuperLimb system with an LQR controller is LAS stable when steps are not being taken. Footstep timing and location paired with a re-computation of the LQR controller make the system into a switched, hybrid system. We propose a way to constrain the switching by using Lyapunov functions to guarantee that the system is stable in the sense of Lyapunov during crawling.

Stability is maintained by commanding steps that keep the system's state in the region of attraction (RoA) of the successive linear controllers. We ensure this by solving for a local Lyapunov [24] function $V(X)$ and then commanding

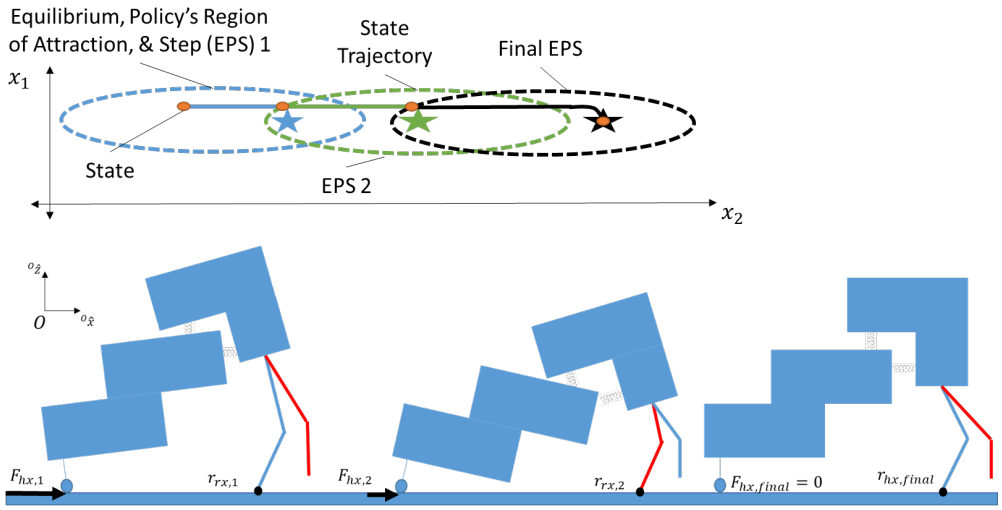

Fig. 3. Schematic illustrating how SuperLimb steps ($r_{rx,i}$) and the re-computation of the LQR policy is synonymous with the system's state moving between adjacent regions of attraction in state space. The top image shows a 2-dimensional phase portrait to allow for easy visualization of the below image's state trajectory. The states x_1 and x_2 of the top image are conceptual aids that allow us to draw the level-set of the closed loop system in 2D. EPS represents the intermediate equilibrium and region of attraction for each step during the crawl. The dotted line illustrates the level-set of the system, the solid line represents the motion of the state, the star illustrates each equilibrium, and the orange dot represents the location of the state when a step is commanded. F_{hx} is the force applied by the operator's knee during the crawl.

steps that keep the system's state in the region where $V(X)$ is positive definite (PD) and $\dot{V}(X)$ is negative definite (ND). We use the optimal cost-to-go (OCTG) of the LQR policy "$J(X)$" as the Lyapunov function because it is by definition PD. Furthermore, to satisfy the Hamilton-Jacobi-Bellman equation $J(X)$ must also satisfy,

$$\frac{d}{dt}\left(J(X)\right) = -(\Delta X^T \cdot Q \cdot \Delta X + \Delta U^T \cdot Q \cdot \Delta U) \quad (9)$$

Thus, we know that $\dot{J}(X)$ is ND. This means that $J(X)$ is a valid local Lyapunov function for the non-linear system.

$$V(X) = J(X) = \Delta X^T \cdot S \cdot \Delta X \quad (10)$$

A. POSITION CONTROL

A summary of the algorythm is shown in Fig. 3. Steps are commanded so that the state remains in the RoA of adjacent, intermediate equilibrium until it reaches the final equilibrium, which corresponds to $x_{h,desired} = x_{h,equilibrium}$. This describes a position controller, because in this formulation $\dot{x}_{h,desired} = 0$. We now explain the policy in more detail.

The SuperLimbs compute a linear controller about the system's first intermediate equilibrium using Eqn 4, and pulls the state towards it. As the system reaches the intermediate equilibrium the Lyapunov decrease monotonically to zero. This equilibrium is not guaranteed to have $x_{h,desired} = x_{h,equilibrium}$, however. This position error is undesirable, so the crawling policy commands steps to move the state between equilibrium until $x_{h,error} = 0$.

First we compute the final position of the foot $r_{ft,x,final}$, which makes $x_{h,error} = 0$. We then solve for the value of $V(X)$ immediately after a candidate step is taken from r_{ft,x,t^-} to r_{ft,x,t^+}. This value is denoted by $V_{t^+}(X)$, and is a function of r_{ft,x,t^+} because the foot position is one of the parameters of Eqn 3.

Because steps are modeled as being impact free the state remains continuous, although not smooth. This means that $V_{t^+}(X)$ is,

$$V_{t^+}(X) = \Delta X_{t^+}^T \cdot S_{t^+} \cdot \Delta X_{t^+}. \quad (11)$$

$$\Delta X_{t^+} = X - X_{eq,t^+}.$$

S_{t^+} is the post-step solution to the CARE equation.

$V_{t^+,max}$ is the critical level set that defines the boundary of $V_{t^+}(X)$. This means that $V_{t^+}(X) < V_{t^+,max}$ is a sufficient condition on switching to guarantee stability of the post-step initial conditions. $V_{t^+,max}$ can be computed in closed form or computed numerically, as discussed in section V.

We choose the largest step that constrains $V_{t^+}(X) < V_{t^+,max}$ and $r_{ft,x,t^+} \leq r_{ft,x,final}$, and then take repeated steps while keeping this satisfied until $r_{ft,x,t^+} = r_{ft,x,final}$.

The scalar guard function $\phi(X)$ triggers a new step when $V(X)$ is close to zero.

$$\phi(X) = V(X) - \epsilon_1. \quad (12)$$

ϵ_1 is a threshold that is chosen heuristically to be $0 < \epsilon_1 << V_{t^+,max}$. This allows us to take a step that changes $V(X)$ by,

$$\Delta V(X) = V_{t^+}(X) - V_{t^-}(X) \approx V_{t^+,max}. \quad (13)$$

This is the largest possible guaranteed stable step, since the step size is proportional to $\Delta V(X)$. Fig. 9 shows a plot of V during a crawling simulation.

It is advantageous to take large steps because we assume that impulsive forces are negligible, but in practice they may

not be. Minimizing the number of steps also minimizes the number of opportunities for the system to depart from the modeled behavior.

B. FULL STATE CRAWLING POLICY APPLIED TO EXAMPLE PROBLEM

We explain the full state policy using a single axis toy problem to ensure that its operation is clear. See Fig. 4 for a schematic of the toy problem.

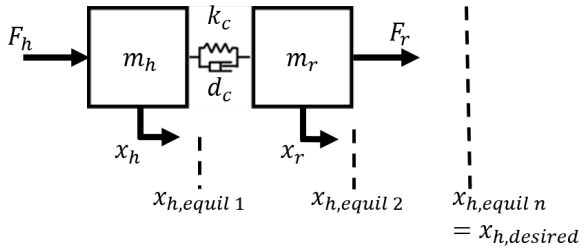

Fig. 4. This is a toy system used to illustrate the functionality of the full state crawling policy.

Here, F_h and F_r represent the force applied by the human and SuperLimbs respectively. k_c, d_c, m_h, and m_r represent the interface compliance and inertial properties of the system. $x_{h,Equil_i}$ are the intermediate equilibrium that we choose for the human's position between his initial state and his desired state, $x_{h,desired}$. $x_{r,Equil_i}$ is the intermediate equilibrium for the SuperLimb's state. The system is assumed to have n intermediate equilibrium until it reaches the desired state.

The human applies the smooth force profile shown in Eqn 14 to move towards $x_{h,desired}$.

$$F_h = k_p * (x_{h,desired} - x_h). \tag{14}$$

k_p is the gain on the force controller. The equations of motion for this simple system are linear and of the form,

$$\dot{X} = A \cdot X + B \cdot F_r. \tag{15}$$

$$F_r = K_{LQR_i} \cdot \Delta X_i + F_{r,equil_i} \tag{16}$$

$$\Delta X_i = (X - \begin{bmatrix} x_{h,equil_i} \\ x_{r,equil_i} \end{bmatrix}) \tag{17}$$

The exact form of A and B are unimportant. K_{LQR_i} is the gain computed using a linear quadratic regulator on the state error ΔX_i. K_{LQR_i} is a function of the system parameters, A and B, by virtue of the LQR formulation. $F_{r,equil_i}$ is the equilibrium force applied by the SuperLimbs at each intermediate equilibrium $[x_{h,equil_i}, x_{r,equil_i}]$.

This simple closed loop system is globally asymptotically stable, so the intermediate equilibrium $x_{h,equil_i}$ can be chosen arbitrarily. $x_{h,equil_i}$ is then used to solve Eqn 15 for $x_{r,equil_i}$ and $F_{r,equil_i}$.

Finally, the progress of the state between intermediate equilibrium is tracked using the Lyapunov function,

$$V(X) = \Delta X_i^T \cdot S_i \cdot \Delta X_i. \tag{18}$$

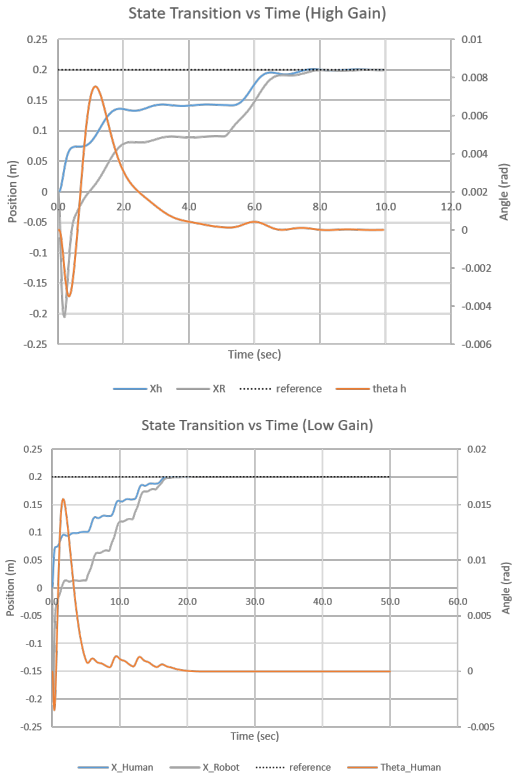

Fig. 5. Translations of the bodies during crawling while using the full state control policy for high (Top) and low (Bottom) gain trials. The maximum step size is limited to .1m to represent the fixed workspace of the SuperLimbs. This constraint is only active during the high gain trial.

S_i is the cost-to-go (CTG) matrix from the LQR policy, and Eqn 18 is the CTG of the system. The CTG satisfies the requirements of a Lyapunov function for each i in $i = 1, .., .n$.

The SuperLimb in Fig. 4 moves the human forward by:

1) Choose a set of intermediate equilibrium $x_{h,equil_i}$, for $i = 1, ..., n$. Where, $x_{h,equil\_n} = x_{h,desired}$.
2) Compute $x_{r,equil_i}$, $F_{r,equil_i}$ and $K_{LQR,i}$ for $i = 1, ..., n$ by using Eqn 15 and standard unconstrained LQR. This implies that the SuperLimb has an accurate estimate of $x_{h,desired}$ and k_p so that it can compute the A in Eqn 15.
3) Compute F_r for $i = 1$ based on Eqn 16, and apply this force to the system.
4) Wait until $V(X) \approx 0$, then increment i. Repeat step 3 with $i = i + 1$ until $i = n + 1$.

This process is essentially the same process used for locomotion of the full system in Fig. 2. The first difference is that the full system is non-linear, so the intermediate equilibrium can not be chosen arbitrarily. Instead we choose them using a Lyapunov function. The second difference is that the full system increments i by taking a step. When a step is taken we change the equations of motion. This is equivalent to changing A when i is incremented.

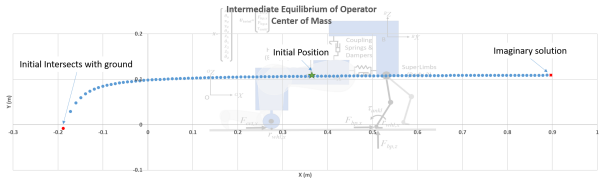

Fig. 6. Intermediate equilibrium of the full state gait policy becoming infeasible due to a reference position that changes too aggressively.

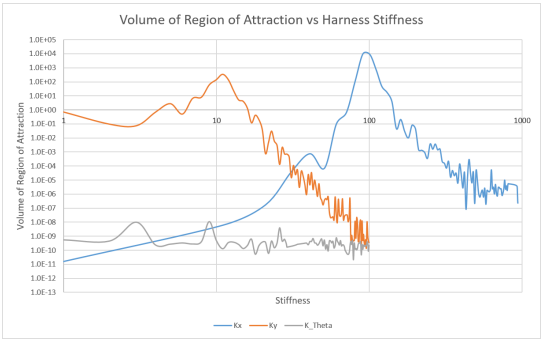

Fig. 7. Log-log plot of the volume of the system's region of attraction as a function of the interface stiffness. The trace is not smooth because $V_{t+,max}$ is estimated numerically.

V. SIMULATION RESULTS

A. VALIDATION OF FULL STATE GAIT POLICY

We simulated the full state policy using the parameters given in Appendix VIII-A. Fig. 5 shows the evolution of the statefor different gains and Fig. 9 shows the Lyapunov function during the low gain trial. Each increase in V coincides with the SuperLimbs taking a step. Because $V_{t^+} < V_{t^+,max}$, $V(t) \to 0$ as $t \to 0$. This coincides with the state converging to the intermediate equilibrium and thus the human moving closer to their desired position.

Fig. 5 shows that with this policy the SuperLimbs take a nearly constant step size, for a given trial, as they approach the desired position. This is because the step size is determined by the maximum allowable value of the Lyapunov function, and this threshold is roughly constant. Additionally, the settling time of the transients following each step in a trial remain nearly constant.

The settling time is determined by the parameters of the LQR policy. The LQR policy is generated with constant Q and R matrices around the computed system equilibrium. For the trials shown these equilibrium are adjacent to one another, so the policies are also similar. If the penalty on state velocities is increased then we see that the transients are reduced, as we expect. (Fig. 5) As the transient times are reduced the SuperLimbs converge on intermediate equilibrium faster and thus the crawling speed is increased.

As the penalty on the SuperLimb's and operator's rotation rates and orientations are increased the settling time is also rapidly reduced. This is because the system non-linearity comes from the bodies' rotation, so the linear Lyapunov function described in Eqn 10 is only valid "near" equilibrium. As the penalty on rotation is increased the bodies rotate less,

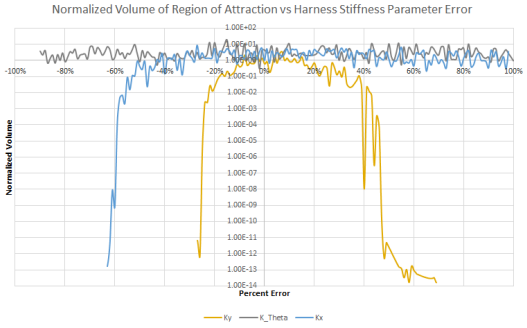

Fig. 8. Semi-log plot of the normalized volume of the system's region of attraction as a function of the percent error in the model's parameter accuracy. Each trace is normalized to the simulation experiment with the correct parameter estimate. See Table II from Appendix VIII-A for the parameters used in this simulation study. The trace is not smooth because $V_{t+,max}$ is estimated numerically.

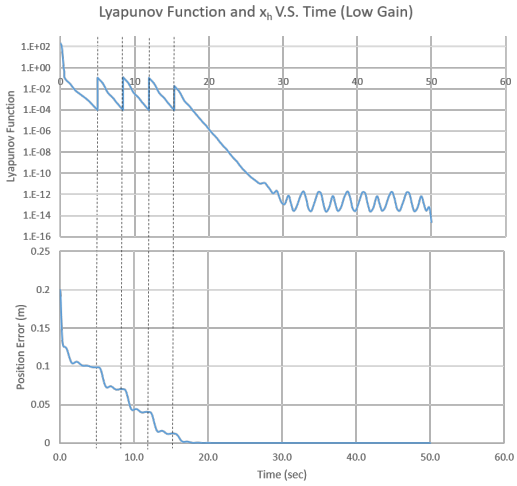

Fig. 9. Plot of the evaluated Lyapunov function versus time for the low gain trial aligned with a plot of the human's reference error. $PositionError = |x_{hd} - x_h|$. The dashed lines indicate when a step is taken. This is why they coincide with discontinuities in V.

and the system model becomes more linear, in a sense. This allows the linear control policy that stabilizes intermediate equilibrium to be more effective, thus reducing the settling time. It also allows the linear Lyapunov function that we define to more effectively represent the system, increasing the threshold value of $V_{t^+}(X)$. A larger $V_{t^+}(X)$ means that the footsteps are larger, Section IV-A, which is equivalent to saying that the intermediate equilibrium can start farther from the current state and still be guaranteed to converge. The impact of increasing the LQR policy's gain is demonstrated in Fig. 10.

The practical upper limit to the speed of the system comes from actuator saturation and the ground's friction cone. This is very different from exo-skeleton systems that have a limited speed/bandwidth based on the interface compliance. We explore other limitations of the full state policy in Sections V-B and V-C.

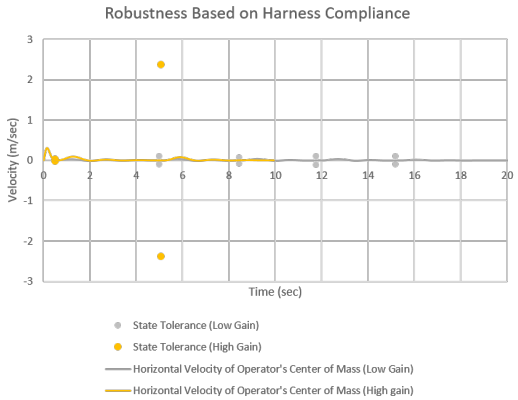

Fig. 10. Plot of the horizontal velocity of the operator's center of mass for low and high LQR policy gain. Each pair of dots is plotted at the time a step is commanded. Their distance from the velocity trace illustrates how much error in that element of the state can be stabilized. This plot shows that the high LQR gain simulation reaches the reference position after two steps, but that the low gain simulation requires five. This also shows that the high gain system reaches the reference in nearly half the time.

B. FAILURE CRITERIA OF FULL STATE GAIT POLICY

The first failure condition occurs when the human reference changes too fast for the SuperLimbs to reach the setpoints. This causes the system's intermediate equilibrium to be too far from its present state. In this situation the computed equilibrium becomes invalid either because it violates geometric constraints, requiring the system to intersect with the ground or exceed reasonable joint limits, or because the equilibrium is mathematically infeasible. Mathematical infeasibility manifests itself as an imaginary solution to the system's equilibrium equations. See Fig. 6 for an illustration of these failure modes.

The second notable failure occurs if the SuperLimb's estimate of the system's parameters, such as the human's desired position, is wrong. In this case the Lyapunov function is an estimate since the control policy would have been based on an incorrectly computed equilibrium. This estimate may not decrease monotonically to zero. Because steps are triggered based on the proximity of $V_{t^-}(X)$ to zero, it is possible for the system to fail to trigger steps as the Lyapunov estimate could fail to decrease enough.

The first concern can be mitigated by training the operator on the system so that they do not attempt to crawl faster than the SuperLimbs can accommodate. The second concern is more worrying because in reality the model of the system will have some error in it, thus the failure mode suggests a strong practical limitation to implementing the policy. This failure mode can be mitigated by using a guard function based on $\dot{V}$ instead of V, and a heuristic step size . This is because the Lyapunov estimate monotonically decays to a constant.

C. IMPACT OF COUPLING COMPLIANCE ON FULL STATE POLICY'S ROBUSTNESS

Interface compliance impacts system stability differently for SuperLimb systems than exo-skeleton systems. This is because the SuperLimbs are coupled to the operator in a fundamentally different way than an exoskeleton, and because it acts independently from their kinematics. We use simulation to explore these trends.

We quantify the impact of interface compliance on the robustness of the full state policy by computing the volume of the system's RoA as we change K and D. If the volume increases this means that the controller is more robust, since we can guarantee that more states are asymptotically stable.

Fig. 7 shows that there is an optimal interface stiffness that maximizes the stability of the system. One reason this is useful is because we assume that ground impacts are negligible, but if in reality they are not and the state velocities are discontinuous after contact then the added robustness of the policy guarantees that the system can recover from the error. We are investigating the physical principle behind the presence of an optimal interface stiffness.

We analyze the algorithm's robustness under parameter error by designing the LQR controller of Eqn 8 based on inaccurate parameter estimates, and then computing the volume of the region of attraction when this erroneous policy is applied to the real system. The result of this analysis is shown in Fig. 8 for the harness compliance parameters. Here we see that the volume of the ROA is far more sensitive to parameter estimation error in K_y than in K_x and K_θ. This implies that LQR formulation makes the control algorithm robust to some errors and sensitive to others.

We have shown a way of modeling the impact of interface compliance on the robustness of the system. One benefit of using LQR to generate the policy is that the system model, including the interface compliance, is used to generate an optimal policy. In this way we account for the compliance to yield an optimal system. The system is therefore optimal for each set of interface parameters, even if these parameters are not the most robust set. This feature is absent from standard exo-skeleton control policies.

VI. CONTRIBUTIONS

We describe a full state crawling policy that guarantees stable locomotion of the Human+SuperLimb system. We also show how the design of the passive coupler can be used to improve the stability of the algorithm.

Many common biped locomotion policies require accurate models of the system dynamics in order to achieve stable locomotion [10], [11]. By formulating the crawling algorithm as described, we are able to design a robust policy that is insensitive to some parameter errors.

The policy architecture is demonstrated on a simple model, but the robust results suggest that a similar method can be used to stabilize more complex dynamic systems. This is the direction of future research.

VII. FUTURE WORK

We have developed a cooperative crawling policy that provides stable locomotion when the state of the human and the dynamics of their crawling controller (Eqn 1) are not available. We will share these results next. We are also

building a reduced scale mock-up of the system in Fig. 2 to validate our contact dynamics assumptions and demonstrate the practicality of the policies. We will also modify the policy to stabilize locomotion for a cart that has intermediate contact with the ground. This will better represent the hybrid dynamics that are seen in crawling. Finally, we expect that un-modeled dynamics such as actuator saturation and friction constraints will result in experimental performance that is somewhat different from our simulated results. This different will likely be due to our use of unconstrained LQR, and our assumption that the system does not violate things such as actuator limits. We will account for this discrepancy by formulating a controller that uses real-time constrained LQR.

VIII. APPENDIX

A.

TABLE I

PARAMETERS FOR THE SIMULATION OF THE FULL STATE CRAWLING POLICY WITH A HIGH CONTROLLER GAIN (TOP) AND LOW CONTROLLER GAIN. (BOTTOM)

$K_{P,Cart} = 9$	$K_{D,Cart} = 0$	$x_{h,des} = .2$	$\dot{x}_{h,des} = 0$
$d_y = 5.8$	$m_h = 1.4$	$m_r = 5.4$	$I_h = 43$
$k_x = 1$	$k_y = 100$	$k_\theta = 10$	$d_\theta = 5.7$
$d_x = 1$	$I_r = 6$		

$K_{P,Cart} = 9$	$K_{D,Cart} = 0$	$x_{h,des} = .2$	$\dot{x}_{h,des} = 0$
$d_y = 1$	$m_h = 1$	$m_r = 1$	$I_h = 1$
$k_x = 10$	$k_y = 10$	$k_\theta = 10$	$d_\theta = 5.7$
$d_x = 2$	$I_r = 1$		

TABLE II

PARAMETERS FOR SIMULATING THE EFFECT OF PARAMETER ERROR ON THE VOLUME OF THE CONTROLLER'S REGION OF ATTRACTION

	K_x Study	K_y Study	K_θ Study
Nominal K_x	100	10	10
Nominal K_y	100	10	100
Nominal K_θ	10	10	10

REFERENCES

[1] G. M. Waehrer, X. S. Dong, T. Miller, E. Haile, and Y. Men, "Costs of occupational injuries in construction in the United States," *Accident Analysis and Prevention*, vol. 39, no. 6, pp. 1258–1266, 11 2007.

[2] Liberty Mutual Insurance, "Liberty Mutual Workplace Safety Index," Tech. Rep., 2018. [Online]. Available: https://business.libertymutualgroup.com/business-insurance/Documents/Services/Workplace Safety Index.pdf

[3] S. Gupta and A. Kumar, "A brief review of dynamics and control of underactuated biped robots," *Advanced Robotics*, vol. 31, no. 12, pp. 607–623, 2017. [Online]. Available: http://dx.doi.org/10.1080/01691864.2017.1308270

[4] S. Kuindersma, F. Permenter, and R. Tedrake, "An efficiently solvable quadratic program for stabilizing dynamic locomotion," *Proceedings - IEEE International Conference on Robotics and Automation*, pp. 2589–2594, 2014.

[5] Q. Nguyen and K. Sreenath, "L1 adaptive control for bipedal robots with control Lyapunov function based quadratic programs," *Proceedings of the American Control Conference*, vol. 2015-July, pp. 862–867, 2015.

[6] E. R. Westervelt, D. E. Koditschek, S. Member, J. W. Grizzle, D. E. Koditschek, and S. Member, "Hybrid Zero Dynamics of Planar Biped Walkers Hybrid Zero Dynamics of Planar Biped Walkers," *IEEE Transactions on Automatic Control*, vol. 48, no. August, pp. 42–56, 2005.

[7] C. Gehring, S. Coros, M. Hutter, M. Bloesch, M. A. Hoepflinger, and R. Siegwart, "Control of dynamic gaits for a quadrupedal robot," in *2013 IEEE International Conference on Robotics and Automation*. IEEE, 5 2013, pp. 3287–3292. [Online]. Available: http://ieeexplore.ieee.org/document/6631035/

[8] H.-W. Park, Sangin Park, and S. Kim, "Variable-speed quadrupedal bounding using impulse planning: Untethered high-speed 3D Running of MIT Cheetah 2," in *2015 IEEE International Conference on Robotics and Automation (ICRA)*. IEEE, 5 2015, pp. 5163–5170. [Online]. Available: http://ieeexplore.ieee.org/document/7139918/

[9] Hirose S., "A Study of Design and Control of a Quadruped Walking Vehicle," *The International Journal of Robotics Research*, vol. 3, pp. 113–133, 1984. [Online]. Available: https://journals.sagepub.com/doi/pdf/10.1177/027836498400300210

[10] H. Kazerooni, R. Steger, and L. Huang, "Hybrid Control of the Berkeley Lower Extremity Exoskeleton (BLEEX)," *The International Journal of Robotics Research*, 2006. [Online]. Available: http://ijr.sagepub.com

[11] H. Kazerooni, J. L. Racine, L. Huang, and R. Steger, "On the control of the Berkeley Lower Extremity Exoskeleton (BLEEX)," in *Proceedings - IEEE International Conference on Robotics and Automation*, vol. 2005, 2005, pp. 4353–4360.

[12] D. A. Kurek and H. H. Asada, "The MantisBot: Design and Impedance Control of Supernumerary Robotic Limbs for Near-Ground Work," pp. 5942–5947, 2017.

[13] N. E. W. Group, "Ergonomics Guide for Welders," no. August, pp. 1–38, 2012.

[14] D. Mien Ka, C. Hong, T. Huu Toan, and J. Qiu, "Minimizing Human-exoskeleton Interaction Force by Using Global Fast Sliding Mode Control," *International Journal of Control, Automation and Systems*, vol. 14, no. 4, pp. 1064–1073, 2016. [Online]. Available: http://dx.http://www.springer.com/12555

[15] H. Kazerooni and S. L. Mahoney, "Dynamics and control of robotic systems worn by humans," pp. 379–387, 1991.

[16] H. Kazerooni, "Human-Robot Interaction via the Transfer of Power and Information Signals," *IEEE Transactions on Systems, Man and Cybernetics*, vol. 20, no. 2, pp. 450–463, 1990.

[17] S. D. Eppinger and W. P. Seering, "On Dynamic Models of Robot Force Control." IEEE, 1986, pp. 29–34.

[18] W. Yu, J. Rosen, and X. Li, "PID admittance control for an upper limb exoskeleton," in *Proceedings of the American Control Conference*, 2011, pp. 1124–1129.

[19] K. Anam and A. A. Al-Jumaily, "Active exoskeleton control systems: State of the art," in *Procedia Engineering*, vol. 41. Elsevier Ltd, 2012, pp. 988–994.

[20] J. E. Colgate, "Robust control of dynamically interacting systems," *International Journal of Control*, vol. 48, no. 1, pp. 65–88, 1988.

[21] S. P. Buerger and N. Hogan, "Complementary stability and loop shaping for improved human-robot interaction," *IEEE Transactions on Robotics*, vol. 23, no. 2, pp. 232–244, 2007.

[22] K. S. Hahm and H. H. Asada, "Design of a Fail-Safe Wearable Robot with Novel Extendable Arms for Ergonomic Accommodation during Floor Work," *Proceedings - IEEE International Conference on Intelligent Robots and Systems*, 2019.

[23] R. P. INC, "The Racatac with Chest Support," 2016. [Online]. Available: https://racatac.com/racatac-with-chest-support/

[24] J.-J. E. Slotine and W. Li, "Applied Nonlinear Control," J. Wenzel, Ed. Upper Saddle River: Prentice-Hall, 1991, ch. 3, pp. 40–95.